Ultrasound Intensified CO_2 Desorption from Pressurized Loaded Monoethanolamine Solutions

I. Parameters Investigation and Modelling

Jiru Ying[1,*], Dag A. Eimer[1,2], Frode Brakstad[1], Hans Aksel Haugen[1]

[1] SINTEF Industry, Porsgrunn 3918, Norway

[2] University of South-Eastern Norway, Porsgrunn 3901, Norway

Abstract

CO_2 stripping from loaded monoethanolamine (MEA) aqueous solutions intensified by means of ultrasound was investigated in a lab-scale kettle reboiler with both gas and liquid continuous operation. The reboiler operating conditions were similar to those of a typical industrial reboiler with a pressure of 1 barg, and where the CO_2 loading is less than 0.25 mol CO_2 /mol MEA. Intermittent ultrasound application was tested to find the effects of variables for CO_2 stripping from the CO_2 loadings 0.20 to 0.39 mol/mol at pressures up to 1.5 barg. Multi-variate data analysis was employed, and a model was built to explain and find the effects of six variables on CO_2 stripping by ultrasound. The six variables include pressure, liquid flow rate, CO_2 loading, intensity, frequency and on-stream time of ultrasound. The variable analysis results manifest that the CO_2 loading is the significant positive effect variable, pressure is negative on energy saving and CO_2 stripping rate and ultrasound parameters have varied effects. Experimental results show that the CO_2 stripping rate assisted by ultrasound is 4 times than by heat only when CO_2 loading is high, and the best result of specific energy consumption was 2.3 MJ/kg CO_2 in the present test conditions.

Keywords: Ultrasound; CO_2 desorption; Loaded MEA aq. solution; Specific energy consumption; CO_2 stripping rate; Lab-scale kettle reboiler

1. Introduction

CO_2 capture and utilization/storage (CCS or CCUS) attract more and more attention due to the problem of global warming. At present, the most mature technology for CO_2 capture is an MEA-based capture technology, which has a high cost, partly due to the energy demand related to the desorption process.

Ultrasound enhanced CO_2 stripping could be one method to unlocking CCS cost savings. Ultrasonic waves have frequencies above 20 kHz making them inaudible. Ultrasound is a mature technology and is widely used in various fields. With respect to the frequency, ultrasound is divided into three categories: power ultrasound (20 – 100 kHz), which is used in chemically important systems; high frequency ultrasound (100 kHz – 1 MHz), which is used for animal navigation and communication, detection of cracks or flaws in solids, and under water echo location; and diagnostic ultrasound (1 – 500 MHz), used as a diagnostic in the medical field.[1-3] In sonochemistry, ultrasound with a frequency ranging from 20 to 100 kHz is used to increase the reactivity through cavitation.[2-4] Cavitation bubbles in the liquid may grow larger than 100 μm through a series of compression and expansion cycles caused by the acoustic waves. Cavitation bubbles can be unstable and implode, producing high-speed liquid micro-jets, localized intense heating and high-pressure shock waves. The expelling liquid jet can move up to speeds of 400 km/h, the hot spots in the cavity can reach thousands of degrees Celsius and the shock waves have been shown sufficient to cleave polymers by mechanical breakage of the chains.[5] Thereby, the effects by cavitation can produce sufficient intensity to enhance chemical reactions and associated mass transfer. Ultrasound is also employed for degassing: removing air from distilled water in laboratory and or hydrogen from aluminum alloy process.[6]

In recent years, ultrasound started to be introduced in gas purification: for stripping acid gas from loaded solutions, for absorbent regeneration and reducing degradation of absorbents. The major mechanisms for improving the mass transfer are the millions of cavitation bubbles that increase the interfacial area between gas and liquid. The micro- liquid jet and vortex produced by ultrasound can increase mass transport as well. For degassing purposes, the frequency of ultrasound is often relatively low (e.g. 20 – 60 kHz) to avoid degradation of the absorbents. Gantert et al.[7] introduced ultrasound to degas CO_2 from amine solutions between 60 to 80 °C under room pressure. They found that CO_2 can be degassed at temperatures lower than 80 °C using ultrasound and appropriate absorbents, and there is no significant difference between desorption at 37.5 kHz and 25 kHz. Xue et al.[8] studied the desorption of sulfur dioxide from citrate solution using ultrasound with frequencies of 20, 40 and 60 kHz. They found that the use of ultrasound can improve the desorption efficiency of sulfur dioxide. Zhang et al.[9] reported a positive influence of ultrasound on the CO_2 desorption rate from a thermomorphic biphasic solvent (TBS). The frequency was fixed at 37 kHz in their investigation. Tanaka et al.[10] investigated the use of ultrasound to remove CO_2 from monoethanolamine (MEA) aqueous solutions in an ultrasound bath with a frequency of 28 kHz at 25 °C. In the above works,[7-10] researchers attempted to enhance CO_2 desorption at lower temperature and tried to look for chemical effects introduced by ultrasound., In our previous work,[11] we introduced

ultrasound to strip CO_2 from amine solutions with high CO_2 loadings at various temperatures under ambient pressure, and found that most ultrasound energy was used for heating but not for stripping when the desorption temperature was low, because ultrasound did not decompose the carbamate by taking on a catalyst role. We also found that the fractional improvement in the CO_2 desorption rate by using ultrasound at lower temperature, is much slower than at high temperature, resulting in a higher energy consumption per unit of CO_2 desorbed at low temperature. Stripping CO_2 by means of ultrasound at low temperature does not seem to be feasible.

However, all these studies were performed at ambient pressure. In a typical MEA-based CO_2 capture plant, the pressure in the reboiler is about 1.0 barg. Ultrasound and its effect on desorption of CO_2 at pressurized conditions has not previously been researched in depth, and a full theoretical model is not available. Previously,[12] preliminary work has been done to investigate the influence of pressure on CO_2 stripping at a pressure range 0 to 1.5 barg with two different pressure control methods. In this work, the ultrasound intensification effects of using ultrasound intermittently were investigated at varying pressures up to 1.5 barg at the boiling point of lean MEA aqueous solutions with CO_2 loadings from 0.2 to 0.4 mol/mol. The conditions were chosen to be representative of an industrial process. Steam heating was employed in the reboiler to simulate industrial conditions. The parameters studied were pressure / temperature, liquid flow rate, intensity of ultrasound, frequency of ultrasound, percentage on-stream time of ultrasound, and CO_2 loading. When in the reboiler, temperature and pressure are thermodynamically connected, and it was elected to use the temperature as the variable when analyzing the data produced.

2. Theoretical Background

The interfacial area between gas and liquid, here manifested by the amount and size of bubbles, plays a key role in any process that involves mass transfer between gas and liquid. Under desorption conditions bubbles are particularly important in that they provide a mass transfer surface for gas that is still physically dissolved in the liquid but lacks the additional energy to form a bubble. This is because the inwards acting surface force and surrounding pressure are very large for a very small bubble,[2, 13] and an incipient bubble is liable to collapse unless it increases to a critical size. In equilibrium, the pressure balance of a bubble and the surrounding liquid is:

$$P_{\mathrm{liq}} + P_{\mathrm{s}} = P_{\mathrm{CO2}} + P_{\mathrm{vap}} \qquad (1)$$

here, P_{liq} is the liquid pressure at the depth of the site, P_{s} is the pressure caused by surface tension, P_{CO2} is the partial pressure of CO_2 in the bubble and P_{vap} is the solvent vapor pressure in the bubble.

When P_{liq} decreases, the volume of the bubble will increase because the pressure inside the bubble is higher than on the outside. On expansion, both P_{CO2} and P_{vap} inside the bubbles become lower, and the driving force of CO_2 diffusing into the bubble becomes higher. Similarly, when the pressure increases continuously bubbles will reduce in size and could finally collapse.

A larger bubble is easier to inflate than a smaller one as evident from equation (2). The additional pressure due to the pressure caused by surface tension is inversely proportional to bubble size. For a spherical bubble with radius R, this Laplace pressure is given by:[2, 13]

$$P_s = \frac{2\sigma}{R} \quad (2)$$

where σ is the surface tension of the liquid.

Once a bubble begins to grow, the pressure due to the surface tension reduces, so the bubble expands rapidly. Ultrasound produces many cavitation bubbles large enough to grow compared to the very small sized heterogeneous/homogeneous bubbles formed when applying heat only.

Ultrasound enhances the mass transfer of gas from liquid phase to gas phase by providing cavities that can accommodate gas molecules such that more gas can be desorbed without being retained in a saturated, or even supersaturated, liquid. According to Schueller & Yang[14], ultrasound makes bubbles form more easily, and the activation energy for surface diffusion decreases. This results in a lower energy consumption for CO_2 stripping. Ultrasound also produces micro-streams and vortices that can intensify the mass transfer in the liquid.

The chemical reaction of CO_2 desorbed from MEA aqueous solution by heating can be described by the following chemical equations.[15-16]

Carbamate converts to carbon dioxide:

$$RNHCOO^- + RNH_3^+ \leftrightarrow 2RNH_2 + CO_2\ (aq.) \quad (3)$$

Ionization of water:

$$2H_2O \leftrightarrow H_3O^+ + OH^- \quad (4)$$

Bicarbonate reversion to carbon dioxide:

$$HCO_3^- + H_3O^+ \leftrightarrow 2H_2O + CO_2\ (aq.) \quad (5)$$

Furthermore, to the extent that carbonate (CO_3^{2-}) is present, it will react with H_2O according to equation (6) to form bicarbonate (HCO_3^-). Carbamate may also be converted to bicarbonate (hydrolysis reaction) through equation (7):

$$CO_3^{2-} + H_3O^+ \leftrightarrow HCO_3^- + H_2O \quad (6)$$

$$RNHCOO^- + H_2O \leftrightarrow RNH_2 + HCO_3^- \quad (7)$$

The CO_2 produced from the chemical reactions will accumulate in the solution if it is not transferred to the gas phase according to:

$$CO_2\ (aq.) \leftrightarrow CO_2\ (g) \quad (8)$$

In principle, the application of ultrasound does not change the thermodynamics of the system in this method. Free gas ready to escape must be available. This requires a certain degree of

supersaturation. In desorption, this will be the case since CO_2 is travelling from its state of being chemically absorbed via a state of physical absorption in the liquid and finally transferring to the gas phase. The equilibrium relations in an amine absorption / desorption system is illustrated in Figure 1.

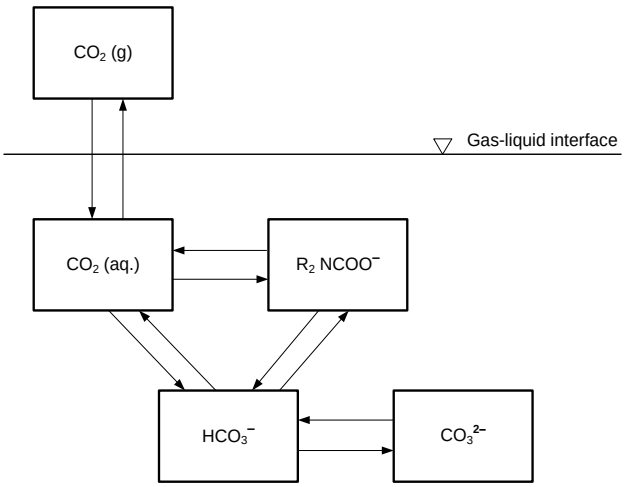

Figure 1. Equilibrium relations in an amine + CO_2 system.

The principle of ultrasound assisted CO_2 stripping is to enhance the transfer of CO_2 (aq.) from the liquid to gas phase, i.e. CO_2 (g). In the solution, the free CO_2 diffuses to the existing bubbles. Therefore, the number of bubbles and the CO_2 partial pressure inside the bubbles are important parameters for CO_2 stripping. The major effect of ultrasound is to produce millions of cavitation bubbles. These bubbles are vacuum bubbles and very small at beginning, the small sizes of the bubbles provide a huge surface area, and the vacuum state of the bubbles cause a large driving force of CO_2 transfer from liquid to the bubbles. The bubbles and turbulence produced by ultrasound will help more of the already "freed" CO_2 in the liquid to desorb instead of staying physically dissolved and re-absorb when the solution is cooled and returned to the absorption section. Ultrasound intensifies the conversion of CO_2 (aq.) to CO_2 (g). Furthermore, the chemical reactions to free CO_2 (aq.) accelerate because the amount of free CO_2 in solution is decreased.

If there is no agitation, most of the produced "free" CO_2 accumulates in the liquid and slowly builds a gas-liquid equilibrium. A prerequisite for gas escaping from a liquid to a gas is that bubbles are formed. Once formed, it is relatively easy for bubbles to grow as more gas diffuses to the bubbles and becomes part of the bubble. Ultrasound also enhances bubble growth through the processes of rectified diffusion and acoustic streaming.[17] Coalescence of small bubbles will further enhance the gas' ability to rise to the liquid surface, which can also be accelerated by ultrasound through Bjerknes forces.[18]

In relation to the classic amine-based absorption-desorption process used to capture CO_2 from a gas, any gas, it should be clear that the actual escape of gas is one of the rate limiting factors in the desorption process. The reboiler in particular, although there is significant bubbling already, contains liquid with a rest content of CO_2 that struggles to reach the gas phase for reasons stated above. If

applied in an efficient way, i.e., ultrasound should not be used as general heating input, ultrasound will help to release this CO_2 and not just heat the liquid. At the high temperatures found in the reboiler, the reaction creating CO_2 from carbamate is fast enough to make more "free CO_2" for the ultrasound to work on.

Because both the chemical reaction of producing CO_2 and the physical desorption of CO_2 from liquid are endothermic, heat input is required for CO_2 stripping. The reboiler can provide simultaneous heat input and mass transfer. Typically, the CO_2 loading in the reboiler is around 0.25 mol/mol. The eventual CO_2 absorption capacity of the solution will be increased, and energy consumption can be reduced if the CO_2 loading becomes lower because of ultrasound introduced. After all, CO_2 (aq.) has already been released from the chemically bound state and needs less energy to desorb. For the reasons explained, the present study looks at the potential for application of ultrasound installed in the reboiler to enhance CO_2 desorption.

3. Experimental Section

3.1. Reagents and Solution Preparation

Reagent grade MEA with mass fraction purity $\geqslant$99.5% was obtained from Merck and used without further purification. Deionized water (purified with an ELGA Purelab Prima 7, Resistivity more than 0.05 MΩ-cm) and MEA were mixed in a tank to produce 20 L of 30 wt% MEA aqueous solution. This solution was loaded by bubbling CO_2 (purity $\geqslant$ 99.995%, from AGA Gas, Norway) through 3 sinters from the bottom of the tank with a CO_2 flow rate of $3.3\ 10^{-5}\ m^3/s$ to prepare expected loading. The CO_2 loading was determined by a density method[12] before the experiments.

3.2. Experimental Equipment and Procedures

The rig was constructed based on a concept where the specific energy input to the kettle reboiler in W/L is the same as that for a typical industrial unit used for CO_2 desorption. Use of steam as heating medium is chosen to be as close to industrially relevant surface temperatures on the heating tubes as possible. A simplified flowsheet of the rig is given in Figure 2.

In the process, a glass kettle reboiler (QVF 5 L, Germany) (4) is fed by rich amine solution from a 20 L feed tank (1) via a gear pump. The rich amine solution is preheated by a heat unit (3) to an expected temperature before it enters the reboiler (4). Boiling is facilitated by steam coming from a 2 kW electrically driven steam generator (Infinity Fluid Co., USA) (12), and the condensed steam is controlled by a steam trap (13) and is collected in a receiving tank (14). This condensed steam is weighed by a balance (15) for the calculation of the energy consumption. The amine solution inventory in the reboiler is kept at approximately 3 liters and controlled by an overflow mechanism. The lean amine flows to a receiving tank (6) via a buffer volume behind the baffle in the reboiler (4). The overhead vapor/CO_2 in the reboiler leaves via a condenser (7) where the water and amine vapors are removed before the flow of stripped CO_2 is measured by a gas flow meter (Alicat M-50, USA) (9). The condensed vapor (water and amine) are collected and weighed for the final calculation of the

energy consumption before being returned to the lean solution tank to avoid a change of concentration of the amine solution.

The reboiler system can be operated under pressures ranging from 0 to 1.5 barg, and the pressure in the reboiler (4) is automatically controlled by a pressure control gauge (17) and a solenoid valve (8). The liquid flow rates are controlled by needle valves (5-1) and (5-2), and monitored by a flow meter (2-1) and (2-2) to keep a constant inventory of liquid in the reboiler. Heat losses to the surroundings are controlled by placing the reboiler (4) in a temperature-controlled oven. All steam pipes out of the oven are thermally insulated to reduce heat loss.

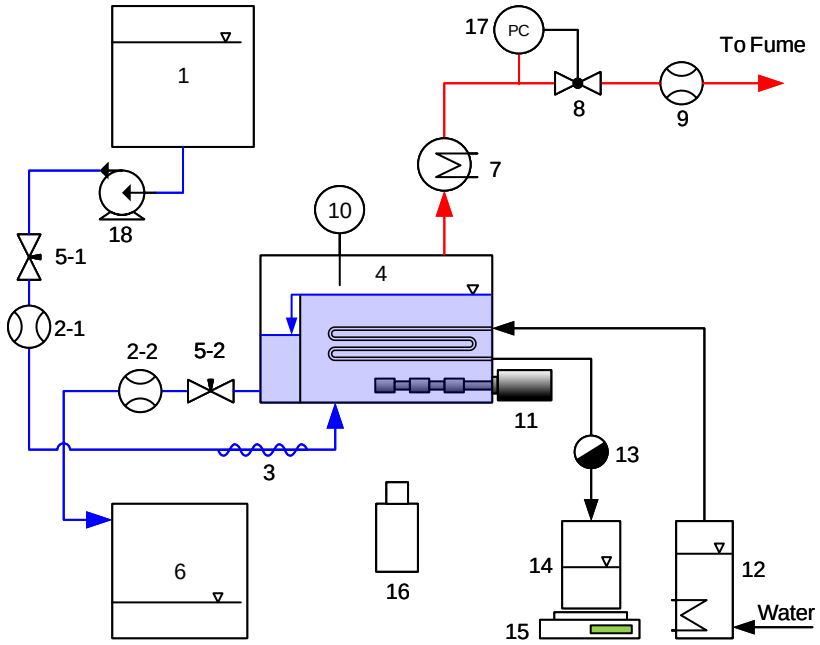

Figure 2. Schematic diagram of the rig used to study ultrasound-enhanced CO_2 stripping from amine solutions. 1, Rich amine feed tank; 2, Liquid flow meters; 3, Preheat unit; 4, Glass kettle reboiler; 5, Needle valves; 6, Lean amine receiving tank; 7, Gas-liquid separator; 8, On-off solenoid valve; 9, CO_2 flow meter; 10, Various sensors (P, T) in liquid and gas; 11, Ultrasound unit; 12, Electric steam generator; 13, Steam trap; 14, Condensed steam receiving tank; 15, Analytical balance; 16, High speed camera; 17, Pressure control gauge; 18, Pump. (Blue lines are liquid phase and red lines are gas phase)

An ultrasound sonotrode (11) is installed at the bottom of the reboiler (4) below the steam heating coil. The ultrasound device (11) was provided by Banry Ultrasonic Co. China. It can be set to 3 frequencies (20, 25 and 28 kHz), and the maximum power output is 500 W. The ultrasonic sonotrodes include two types for each frequency: one is multi-surface type, the other has normal cylinder shape (see the supporting information). The energy input of the ultrasound is calculated using an ammeter.

All the data of flows, temperatures and pressures were recorded by a data acquisition system (Agilent 34972A). Each experiment was run 4-6 min and the data were logged when the process was stable. A high-speed camera (16) is placed in the front of the reboiler (4) for recording the experimental phenomena.

3.3. Typical experimental observation

Figure 3 shows typical curves of pressure, temperature of gas and liquid, stripped CO_2 flow rate when ultrasound is applied, and Figure 4 shows the bubble evolutions in the reboiler corresponding to the moments shown in Figure 3. It can be seen how the liquid is gently boiling as depicted by bubbles rising from the heating tubes before the ultrasound is introduced, (the bubbles are less and small because the boiling bubbles are difficult to form and grow under pressure, see equation (1)), then how ultrasound creates a swarm of bubbles that dominates, rises and disappears after the ultrasound is switched back off; and how the pressure, gas temperature, liquid temperature and flow rate change at different periods. The measured variations of the parameters are shown in Figure 3. Details of bubble observations are given in the captions of Figure 4.

It can be found that the temperature of liquid in the reboiler is relative stable, but the temperature of gas changed with the fluctuation of pressure. The endothermic CO_2 desorption and evaporation of water/MEA were partially compensated for by heat supply from steam. Furthermore, the heat capacities of the liquid and containing equipment dampened any temperature changes. The gas, however, was cooled on expansion and heated on compression without significant dampening. Such compression and expansion are caused by gas release induced by ultrasound and valve opening respectively.

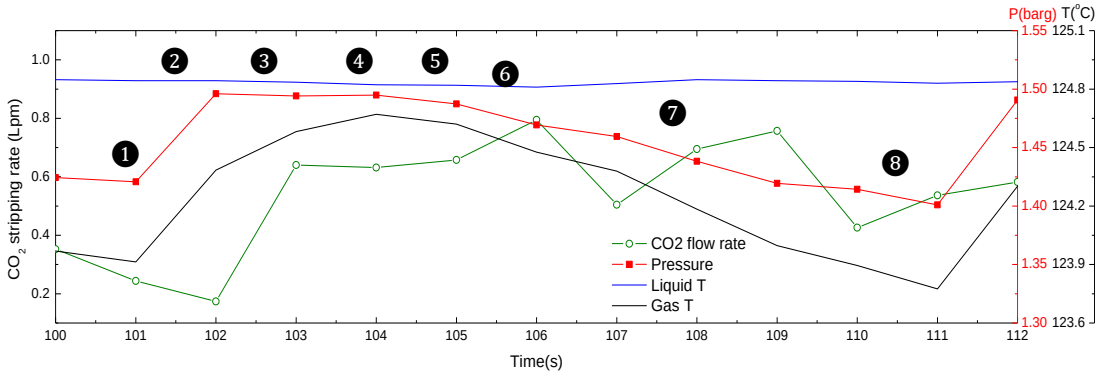

Figure 3. Typical real-time curve of CO_2 stripping rate, pressure and temperatures, ultrasound is employed. (t_{on}: t_{off} = 3:7, 1.45 barg, 0.25 CO_2 loading, 30 wt% MEA).
(The numbers in the figure refer to the moment of the pictures in Figure 4)

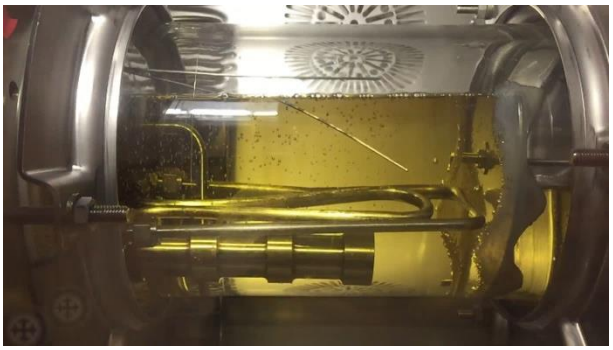

❶ Before the ultrasound is switched on a small amount of bubbles is generated at the heating coil.

❷ Start ultrasound, needle valve (8) opens as the pressure starts increasing, CO_2 is released, cavitation bubbles are growing

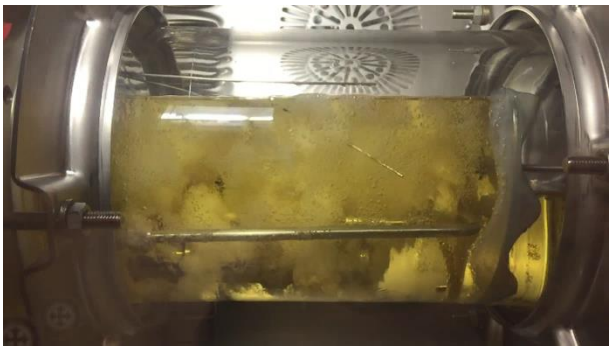

❸ Valve (8) opens, the pressure increases slightly, CO_2 is released, cavitation bubbles are growing and rising

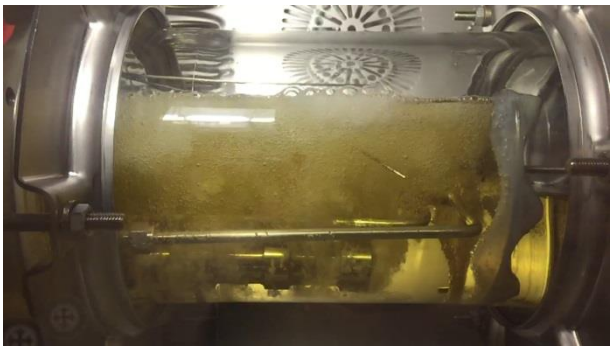

❹ The bubbles continue to grow and rise

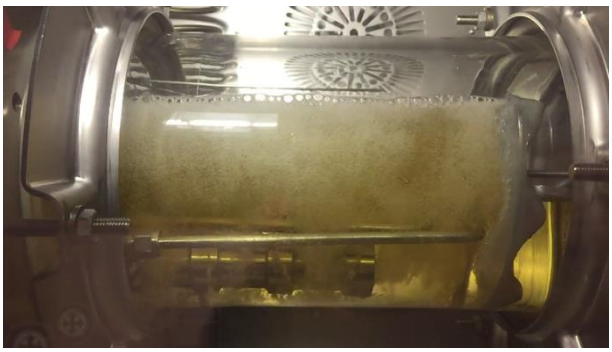

❺ The bubbles continue to grow and rise, but become less

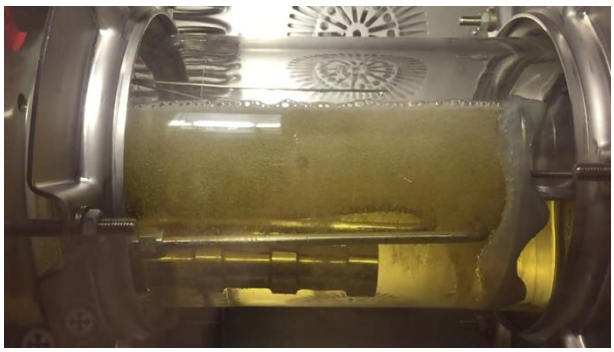

❻ Ultrasound stops, the pressure continues to decrease

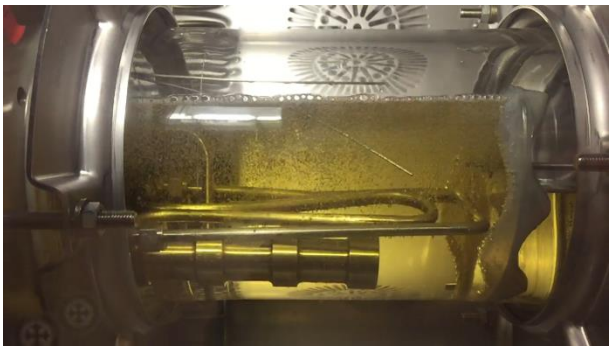

❼ Ultrasound stops, final bubbles rise

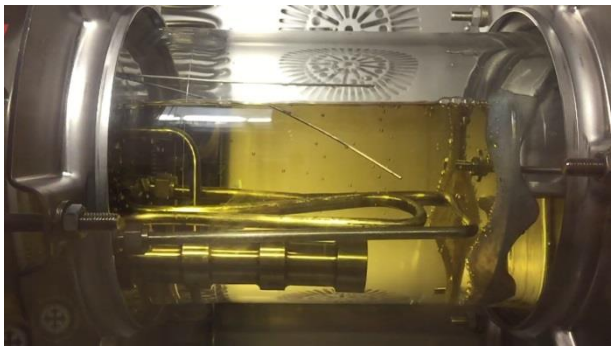

❽ Ultrasound stops, the pressure continues to decrease.

Figure 4. Pictures snapped from the video of one experiment as shown in Figure 3, ultrasound is employed (t_{on}: t_{off} = 3:7, 1.45 barg, 0.25 loading 30 wt% MEA).

It is clear that there is always a pressure surge when the ultrasound is applied. The explanation is that the surge of gas flow is too large for the control system to handle, maybe for any control system in view of the ratio of flow rates. Due to thermodynamics, the pressure surge suppresses boiling by causing a higher boiling point. Since the CO_2 being boiled off is supercritical with respect to temperature, the use of the term boiling point could be debated, but the sum of the partial pressures of the components (CO_2, H_2O and MEA) must still be equal to the total pressure for bubbling to occur. Hence, the bubbling from the heating tubes stops when the pressure increases, see the pictures presented. The question is, what does this halt to bubbling mean for the heat transfer and eventually for the endothermic desorption? Looking at the overall heat transfer coefficients for 1) a steam driven evaporation of organic aqueous solution and 2) a steam heating of the same, it appears that these coefficients are similar and in the range 600 – 1200 W/(m^2·K).[19] From this point of view, the heat input to the solution will not be very different during ultrasound treatment with an ensuing pressure surge. There is also a significant heat buffer in the solution and the hardware. It is likely that the slight fall in liquid temperature observed has more to do with the increased rate of the endothermic desorption than with a decreased heat input.

3.4. Experimental Matrix Design

From previous work,[11] it is known that the concentration of "free" CO_2 in the solution becomes low, and the temperature decreases after ultrasound input. It is necessary to wait for the solution to produce more "free" CO_2 from carbamate by heating. In this work, an intermittent application of ultrasound was employed, a variable. A variable, *t*%, the percentage of on-stream time of ultrasound (t_{on}) in experimental period ($t_{on} + t_{off}$) is defined, and this variable is investigated.

Based on the previous results at ambient pressure[11] and the experimental observations at pressurized conditions, there are six parameters (independent variables) that are investigated, i.e. temperature (*T*), intensity of ultrasound (*I*), frequency of ultrasound (*f*), percentage on-stream time of ultrasound (*t*%), liquid flow rate (*L*), and CO_2 loading (α). A measurement plan suitable for multivariate regression analysis with 19 experiments was made as shown in Table 1. The experimental matrix was constructed according to a 2^{6-2} fractional experimental design.[20] (Here, "2" in the base represents the number of levels each variable is tested at; "6" is the number of variables; "2" in the exponent describes the fraction of the full factorial used). For each variable, a low and high level were set, and the experiments were carried out such that all variable combinations were systematically covered and varied independently of each other. In addition, three replicate experiments on average values of the variables were used to quantify the random variation, and to

1. Ensure that the systematic variation of the variables between the low and high levels were causing an effect in the responses (i.e. validation by prediction), and to
2. Quantify possible non-linearity in the model in between the selected max and min levels.

The frequencies of ultrasound for the three replicate experiments (No. 17, 18 and 19) on average values were set to 24 kHz according to the 2^{6-2} fractional experimental design. However, only a 25

kHz sonotrode is available in our lab, which is close to 24 kHz. Therefore, the 25 kHz sonotrode was used in the three replicate experiments.

Table 1. The designed test matrix with 6 variables.

Exp. no.	run order	T °C	I %	f kHz	t% %	L 10^{-6} m^3/s	α mol/mol
1	13	105	70	20	6	1.67	0.15
2	14	125	70	20	6	6.67	0.15
3	5	105	100	20	6	6.67	0.30
4	4	125	100	20	6	1.67	0.30
5	3	105	70	28	6	6.67	0.30
6	8	125	70	28	6	1.67	0.30
7	9	105	100	28	6	1.67	0.15
8	10	125	100	28	6	6.67	0.15
9	6	105	70	20	50	1.67	0.30
10	7	125	70	20	50	6.67	0.30
11	15	105	100	20	50	6.67	0.15
12	16	125	100	20	50	1.67	0.15
13	11	105	70	28	50	6.67	0.15
14	12	125	70	28	50	1.67	0.15
15	1	105	100	28	50	1.67	0.30
16	2	125	100	28	50	6.67	0.30
17	17	115	85	24	28	4.17	0.23
18	18	115	85	24	28	4.17	0.23
19	19	115	85	24	28	4.17	0.23

In parallel 19 similar experiments were performed without the application of ultrasound (only boiling with steam heat) in order to investigate the enhancement of CO_2 desorption by ultrasound.

Since there could be some uncondensed vapor and aerosols downstream of the condenser, the volumetric measurement of CO_2 desorbed will be affected. To check this, two blank experiments of 30 wt% MEA solutions without CO_2 loading were carried out with ultrasound at 105 °C and 125 °C to allow correcting for this. The gas/vapor flow rate of the blank experiments are 0.04 and 0.09 g/min at 105 and 125 ºC respectively, much smaller values than the value of loaded solution for which a typical value was bigger than 1 g/min. Hence, the effect (error) of uncondensed vapor can therefore be neglected, this effect will be accounted for in the uncertainty analysis. (See the supporting information).

3.5. Definition of respondents / parameters

The measured CO_2 desorption and the derived variables are defined below.

The stripping rate of CO_2, A_{CO2}, in unit g/min, is defined as

$$A_{CO2} = \frac{A}{t} \text{ , (g/min)} \qquad (9)$$

where A is the total weight (in unit g) of stripped CO_2, and t is the experimental time in unit minute.

The specific energy consumption, E_s, in unit MJ/kg CO_2, is defined as

$$E_s = \frac{H}{A_{CO2}}, \quad (\text{MJ/kg CO}_2) \tag{10}$$

where H is the total energy consumption including both thermal and ultrasound (in unit MJ/min) defined as,

$$H = H_{st} + H_{US} - H_{cw} \tag{11}$$

where H_{st} is the energy input into the reboiler from steam, H_{US} is the ultrasound energy input, H_{cw} is the energy requirement for vapor condensed in the condenser H103, this energy is calculated by the flow rate and temperature increase of the cooling water. All the H are in unit MJ/min.

The specific energy consumption of a CO_2 capture plant is based on a drop in CO_2 loading from 0.45 to 0.25 mol/mol and the water (and MEA) vapor rising from the reboiler was utilized to desorb CO_2 in the desorption column. Here these vapors flow out from the reboiler were not used for further stripping like in a traditional desorption column. Further, the CO_2 loadings of the rich MEA solutions in this work were in the range of 0.2 to 0.4 mol/mol. From our previous work, it is known that the CO_2 stripping is very dependent on the CO_2 loading.[11] Therefore, the results of E_s from this work cannot be compared directly to the rules of thumb (e.g. 4.2 MJ/kg CO_2) [21] for an industrial CO_2 capture plant.

The energy saving due to ultrasound introduced, η, in unit %, is defined as

$$\eta = \frac{E_{s,H} - E_{s,US}}{E_{s,H}} \times 100\% \tag{12}$$

where, $E_{s,US}$, is the specific energy consumption when treated by ultrasound + heat; $E_{s,H}$, is the specific energy consumption when treated by heat only.

4. Results and Discussion

Typical CO_2 stripping curves of the measurements, i.e. experiment 6 as an example, are shown in Figure 5. Figure 6 (a) is heat treatment (boiling) only and figure 6 (b) is ultrasound treatment with steam heat boiling. In this measurement. The pressure was set to about 1.5 barg and the corresponding boiling temperature was approximately 124°C. During the measurements, CO_2 was stripped from the solution and this caused the gas phase pressure to increase. When the pressure was higher than the upper-limit pressure set point of the pressure controller, the gas outlet valve opened, and CO_2 was released bringing the pressure down to the lower set point of the valve at which point the valve closed. The pressure in the reboiler subsequently increased again due to CO_2 being desorbed continuously. This process ran in cycle automatically. The bubbling phenomena were similar to Figure 4.

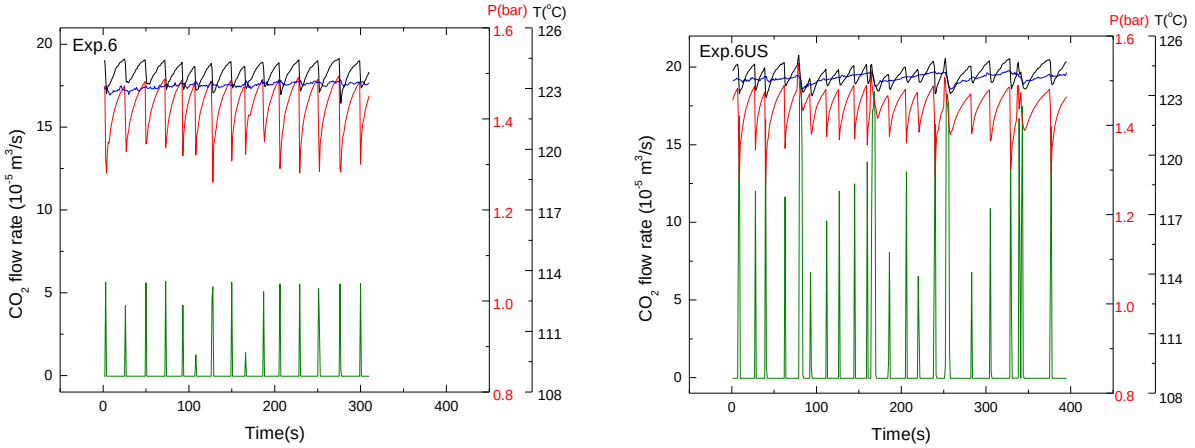

Figure 5. Typical CO_2 stripping curves from the measurements, (e.g. experiment 6). (left, a, boiling with only steam heat; right, b, ultrasound with boiling of steam). The green line (bottom) is the CO_2 flow rate, the red line (middle) is the pressure in the reboiler, the black line (top) is the gas temperature and the blue line (top) is the solution temperature in the reboiler.

It can be seen from Figure 5 that the stripped CO_2 flow rate increased and formed a peak when the gas outlet valve opened, then dropped down to 0 m^3/s as the valve closed. Simultaneously, the pressure and the temperatures of both liquid and gas dropped because CO_2 was released from the reboiler. The gas temperature is more dependent on the pressure and therefore decreased more than that of the liquid. The temperature of the liquid decreased because of the CO_2 endothermic desorption and the evaporation of the liquid. Comparing the two cases we find that the CO_2 stripping rate when treated by ultrasound is much higher than by heat only. For example, exp. 6, about 400% improvement was found by ultrasound treatment (in which A_{CO2} is 1.51 g/min under ultrasound treatment and 0.3 g/min by the treatment of heat only).

Table 2. The results of test matrix 1 derived from experiments.

No.	T	P	α	L	Heat only		Ultrasound + Heat					
					$\boldsymbol{A}_{CO2}$	$\boldsymbol{E}_{s,H}$	I	f	t%	$\boldsymbol{A}_{CO2}$	$\boldsymbol{E}_{s,US}$	η
	°C	bar(g)	mol/mol	10^{-6} m^3/s	g/min	MJ/kgCO_2	%	kHz	%	g/min	MJ/kgCO_2	%
1	105.0	0.06	0.207	1.67	1.77	5.5	70	20	6	1.54	6.8	-24%
2	117.1	1.03	0.207	6.67	0.07	772.0	70	20	6	0.05	976.8	-27%
3	105.1	0.28	0.370	6.67	2.03	12.6	100	20	6	3.09	11.3	10%
4	123.1	1.45	0.390	1.67	1.05	5.1	100	20	6	1.98	20.0	-295%
5	102.3	0.08	0.370	6.67	3.08	7.4	70	28	6	2.89	7.3	1%
6	123.9	1.44	0.321	1.67	0.30	29.4	70	28	6	1.51	3.4	88%
7	105.0	0.06	0.202	1.67	1.45	18.2	100	28	6	1.09	22.7	-25%
8	123.9	1.26	0.208	6.67	0.41	41.1	100	28	6	0.55	198.0	-382%
9	105.0	0.11	0.340	1.67	4.11	4.4	70	20	50	2.64	10.3	-132%
10	121.0	1.40	0.300	6.67	0.18	112.0	70	20	50	0.49	64.4	42%
11	103.7	0.06	0.201	6.67	0.84	60.6	100	20	50	0.76	69.8	-15%
12	124.4	1.17	0.200	1.67	0.81	61.5	100	20	50	0.88	56.5	8%
13	103.1	0.06	0.209	6.67	0.85	46.1	70	28	50	0.86	39.2	15%
14	125.6	1.27	0.209	1.67	0.16	66.3	70	28	50	0.69	24.4	63%
15	106.2	0.25	0.370	1.67	5.17	5.5	100	28	50	4.89	3.9	30%
16	121.2	1.34	0.370	6.67	3.74	3.5	100	28	50	5.39	2.3	36%

Results of the measurements are shown in Table 2. Because the temperatures of the solution and gas decreased with increased gas desorption, it was difficult to control the temperature in the rig at the value stipulated by the test matrix. This led to deviation of temperatures between the matrix design and the actual controlled experiments. The actual experimental conditions are shown in Table 2. The uncertainties of A_{CO2} and E_s are 3.4% and 7.9%, respectively (see the supporting information). It can be seen that the energy saving, η, depends on the operational conditions. Some η values of the experiments (no. 1, 2, 4, 7, 8, 9 and 11) are negative, because there were not enough "free" CO_2 in the solution at these conditions. In these cases, ultrasound introduced was mainly used for heating the solutions then had no positive effect on the energy for CO_2 stripping. These phenomena manifest that should it is wise to keep the ultrasound level low in order to maximize bubbles formation and minimize heat effect for the application of ultrasound. The improvements seen in experiments 6, 10, 14 and 16 are significant, and the E_s is only 2.3 and 3.4 MJ/kg CO_2 at the conditions of experiment 16 and 6 respectively. This is very promising compared with 3.5 and 29.4 MJ/kg CO_2 of the heat desorption.

A higher CO_2 stripping rate means higher CO_2 mass transfer kinetics in the desorption process. It can be seen from Figure 6 that the CO_2 stripping rate is changed significantly with the operating conditions, from close to 0 (exp. 2) and up to > 5 g/min (exp.16). Experiments 15 and 16 show significantly higher CO_2 stripping rates, indicating that strong CO_2 stripping happened when solutions were treated by ultrasound + heat. Experiments 2 and 8 show only little CO_2 stripping by the ultrasound + heat treatment. The consistence between the replicate experiments 17, 18 and 19 is very good. This means repeatability is good.

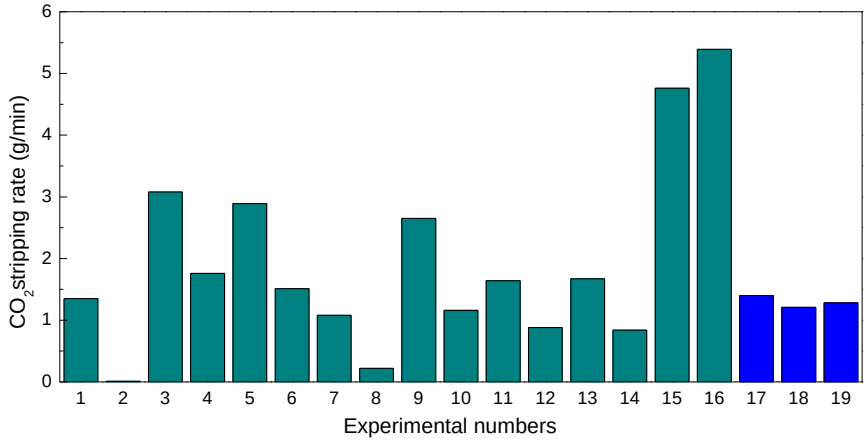

Figure 6. CO_2 stripping rate of the all experiments, A_{CO2}, as dependent variable. The experiments no. 1 - 16 with variables tested at either min or max values, while the blue bars are the 3 replicates run where all variables are at average values.

A lower specific energy consumption was the target. It can be seen from Figure 7 that specific energy consumption E_s is very widely spread with the operation conditions. These experiments stood out with respect to rate of CO_2 stripping, and experiment 16 gave the best result regarding specific energy consumption. This is because there were strong CO_2 stripping happening related to energy input when solutions were treated by ultrasound. The positive results are in agreement with the positive results when A_{CO2} is the dependent variable. Experiments 2 and 8 show very high specific

energy consumption, reaching 976.8 and 198 MJ/kg CO_2. This is because much less CO_2 stripping takes place in spite of the high energy input.

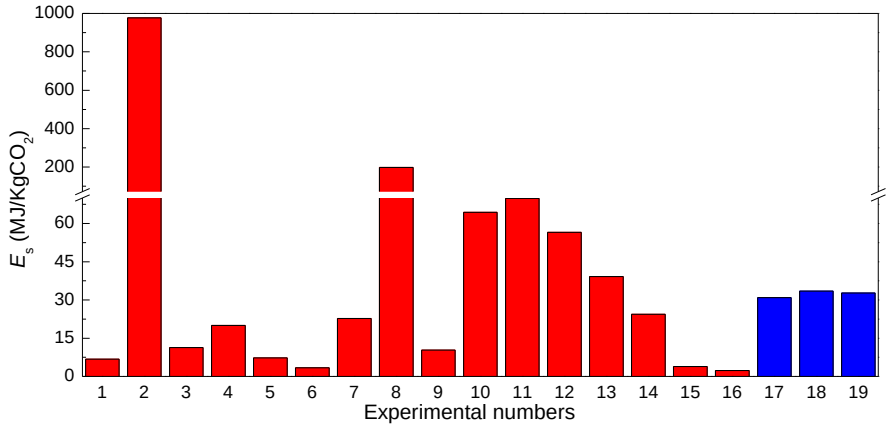

Figure 7. Specific energy consumption, E_s, as dependent variable. The experiments no. 1 - 16 with variables tested at either min or max values, while the blue bars are the 3 replicates run where all variables are at average values.

5. Modelling and Variable Analysis

5.1. Modelling and Correlations

The flow of desorbed CO_2 can be used to represent the outcome of the measurements, but there is also a couple of other possibilities, for examples, A_{CO2}, E_s and η. Only A_{CO2} and E_s were employed for data analysis by statistical methods in this work. A_{CO2} is a kinetics parameter, indicating how fast the mass transfer of CO_2 is. E_s is a thermodynamic parameter, that denotes the specific energy consumption in the process.

The effects of the six independent variables (T, α, L, I, f, and t%) and their interactions on A_{CO2} and E_s were expected to be found by a Partial Least-Squares regression (PLS) method. Even though there are deviations of temperatures between the design test matrix and the actual controlled experiments, the test results can still be analyzed by a PLS method. Regarding the dependent variable, E_s, not all data may be used because the values of experiments 2 and 8 are too high (976.8 and 198 MJ/kg CO_2) due to almost no CO_2 being stripped in these experiments, and these two experiments were classified as strong outliers from the statistical analysis. As a result, these two experiments are overlooked in the present analysis, but could be subjected to new measurements. Because these two experiments were excluded from the modelling of the specific energy consumption, the data were not completely orthogonal anymore, but PLS can handle non-orthogonal (correlated) variables well.[22]

A model explaining 87.5 % of the variation in the rate of CO_2 stripping (A_{CO2}) was obtained by the PLS method, and this model also explains 87.6 % for the specific energy consumption (E_s), see Figure 8. The effects of the interactions between the variables were small and could be neglected. Thus, the correlation equation in terms of the independent variables for the dependent A_{CO2} or E_s is shown in equation (13).

$$A_{CO2}(\text{or } E_s) = a + \sum_{i=1}^{6} b_i x_i + \sum_{i=2}^{6} b_{1i} x_{1i} + b_{24} x_{24} + b_{26} x_{26} + b_{124} x_{124} + b_{126} x_{126} \quad (13)$$

where x_i (i is from 1 to 6) represents the six variables T, α, L, I, f, and t%, respectively. x_{ij} (or x_{ijk}) represents the interaction of variables i and j (and k), for example, x_{13} represents the interaction between variables x_1 and x_3, where x_1 is T and x_3 is L. similarly, x_{124} represents the interaction of variables x_1, x_2 and x_4, where x_1 is T, x_4 is I and x_6 is t%. b_i (or b_{ij} or b_{ijk}) represent the parameters to the related variables. The regressed parameters of the model in equation (13) are shown in Table 3.

Table 3. Regressed parameters of the modelling of equation (13) with 4 significant figures

Parameters	Relevant variables	A_{CO2}	E_s
		Regression coefficients	Regression coefficients
a		-5.842	-361.5
b_1	T	8.629×10^{-2}	2.395
b_2	α	99.27	-510.9
b_3	L	-1.167×10^{6}	1.757×10^{7}
b_4	I	9.390×10^{-2}	-3.601×10^{-1}
b_5	f	-7.199×10^{-2}	12.06
b_6	t%	9.785×10^{-2}	3.582
b_{12}	$T\times\alpha$	-1.079	8.544
b_{13}	$T\times L$	1.008×10^{4}	-1.390×10^{5}
b_{14}	$T\times I$	-1.487×10^{-3}	1.824×10^{-2}
b_{15}	$T\times f$	1.346×10^{-3}	-1.223×10^{-1}
b_{16}	$T\times t$%	-1.180×10^{-3}	-2.052×10^{-2}
b_{24}	$\alpha\times I$	-7.014×10^{-1}	7.280
b_{26}	$\alpha\times t$%	-5.337×10^{-1}	-11.67
b_{124}	$T\times\alpha\times I$	9.378×10^{-3}	-1.135×10^{-1}
b_{126}	$T\times\alpha\times t$%	6.119×10^{-3}	7.529×10^{-2}

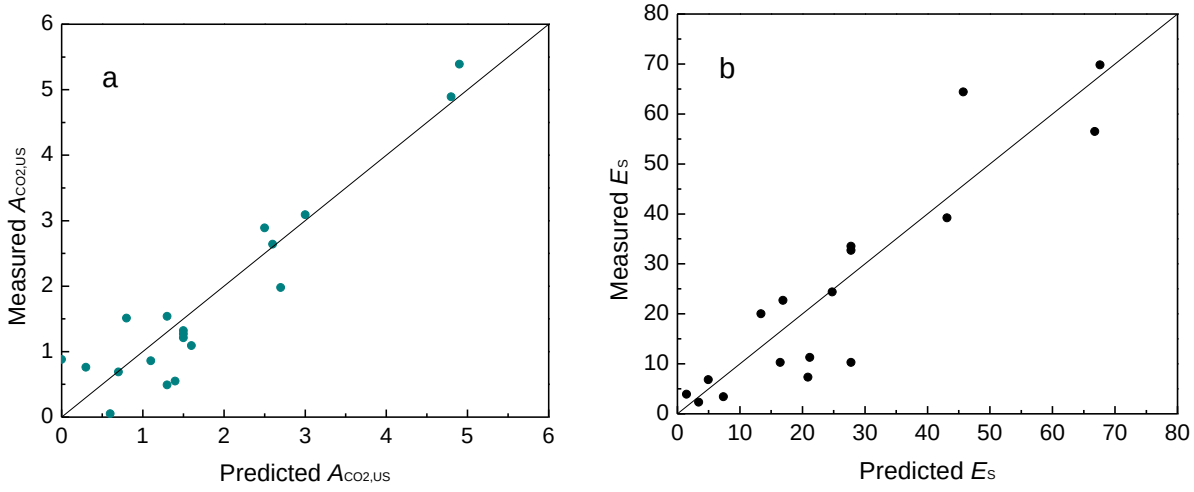

Figure 8. Comparison of measurement and data representation based on equation (13), A_{CO2} (left, a), E_s (right, b)as dependent variable, respectively.

5.2. Variables Analysis

Figure 9 are the contour plots showing the effects of variables α and T (left, a), and variables T and t% (right, b) on CO_2 stripping rate respectively when the other variables were kept on average values. It can be found from Figure 9 (a) that higher CO_2 loading and higher intensity of ultrasound will give a higher CO_2 stripping rate at the top-right corner. Of course, higher intensity of ultrasound means more energy will be put into the solution. This gives the possibility to optimize the operation conditions of ultrasound by modelling and analysis to achieve higher A_{CO2} and lower E_s. It is interesting that the CO_2 stripping rate is almost independent of the intensity of ultrasound when CO_2 loading is lower than 0.224 because of little "free" CO_2 in the solution. It can be found that lower temperature (or pressure) and longer ultrasound running time lead to higher CO_2 stripping rate, as shown in the left side (orange area) of Figure 9 (b). It is noted from Figure 9 (b) that longer ultrasound running time will also cause higher energy consumption. The interesting phenomenon is that the orange area in Figure 9 (b) is not a corner but a curved stripe, this implies that there is also a potential to optimize the T and t% to achieve the highest A_{CO2} and lowest E_s simultaneously.

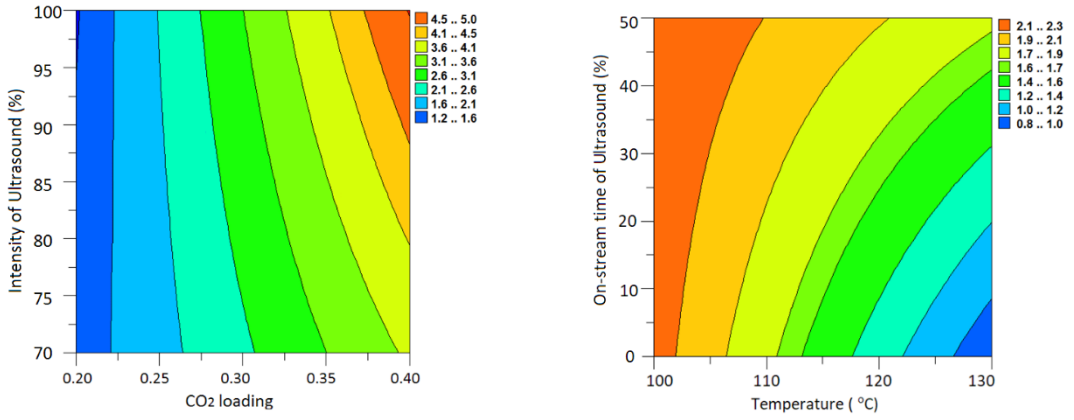

(a) (b)

Figure 9. Simulating the effects on A_{CO2} of Intensity of ultrasound (I) and CO_2 loading (α) (left, a), and Temperature (T) and On-stream time of ultrasound (t%) (right, b). All other variables are kept on average levels.

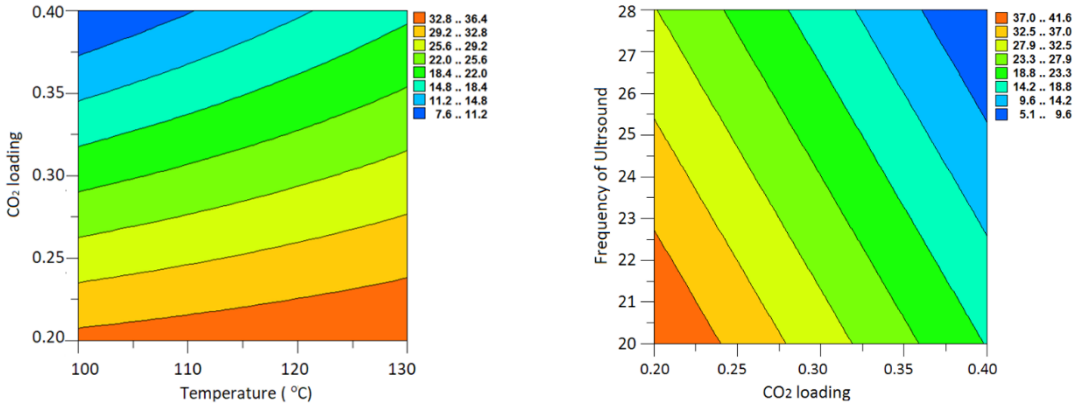

(a) (b)

Figure 10. Simulating the effects on E_s of CO_2 loading (α) and Temperature (T) (left, a), CO_2 loading (α) and Frequency (f) (right, b). All other variables are kept on average levels.

Figure 10 shows the effects of some variables on E_s, it is suggested from both the contour plots that higher CO_2 loading is positive for saving energy, this is the same effect as the result of previous work at ambient pressure. However, it is found from Figure 10(a) that there is a negative effect of temperature on saving energy, i.e. higher temperature causes a higher E_s value. This seems to be the opposite of previous results at ambient pressure. Actually, the temperature parameter is the combined effect of temperature and pressure due to the aqueous solution being at its boiling point in the reboiler, and the liquid temperature is thermodynamically related to the gas phase pressure. Pressure is a significant negative parameter for the CO_2 stripping rate and energy saving because the cavitation bubbles by ultrasound will be depressed by the high pressure and that causes the temperature parameter to become negative. (The temperature is actually a positive parameter for saving energy according to the earlier results at ambient pressure [11]).

It can also be found from Figure 10(b) that higher frequency of ultrasound leads to lower energy consumption. This result is not in agreement with the literature, which claimed that a lower frequency is supposed to cause a higher gas (SO_2) stripping rate.[8] This is probably caused by the different surface areas (or sizes) of the 3 sonotrodes in this work, as shown in Figure 11, the 25 kHz sonotrode is shorter than the 20 and 28 kHz sonotrodes. We did observe that more bubbles were produced from the 28 kHz sonotrode which has a larger surface area. These observations may indicate that the effect of ultrasound frequency is not significant in this small frequency range (20 - 28 kHz), and the active surface area of the ultrasound sonotrode is probably more important.

Figure 11. The sonotrodes used depicted.
Note the different length of the sonotrodes of 20, 25, 28 kHz (the 25 kHz being the shortest)

More contour plots of the effects of variables on A_{CO2} and E_s can be found in the supporting information.

5.3. Which Variables Are Important?

5.4. CO_2 stripping rate as the dependent variable

The relative effects of different variables on the CO_2 stripping rate (A_{CO2}) from the solution were obtained and the results are shown in Figure 12. In the figure, higher absolute value of weighted regression coefficient indicates higher impact on the dependent, and a positive value means the variable has a positive direction for increasing the value of the dependent, i.e. A_{CO2}, and vice versa.

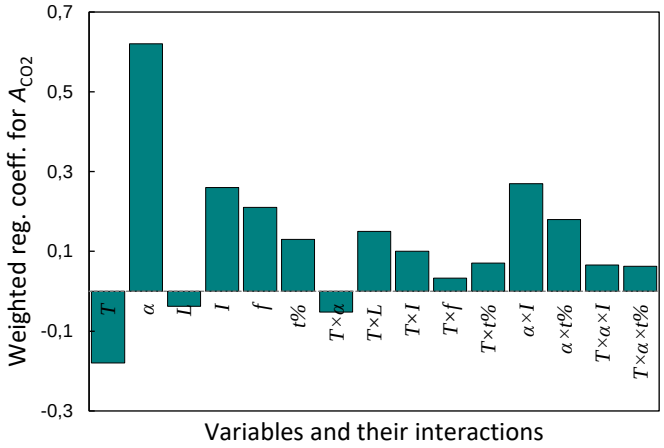

Figure 12. Effects of the variables and their interactions on CO_2 stripping rate, A_{CO2}.

It is shown that the variables and the interactions of T, L and $T \times \alpha$ have a negative effect on A_{CO2}, and the rest of the variables and the interactions have positive effects. Of these effects, the CO_2 loading is the most important parameter (weighted regression coefficient of α is 0.62), with the highest positive influence. Temperature shows a negative effect but not so strong (weighted regression coefficient of T is -0.18), i.e. the higher the temperature, the lower the CO_2 stripping rate is.

The effects of the parameters of ultrasound (I, f and t%) cannot be neglected from the figure, which means there is a potential to optimize the ultrasound parameters to increase the CO_2 stripping rate.

The effect of liquid flow rate is not significant, the following factors may be the reasons affecting the results. Firstly, higher liquid flow rate should cause higher CO_2 loading in the reboiler. However, the lower temperature (approx. 100°C) used in the liquid feed, to avoid flashing of CO_2 on entry to reboiler, has an influence on the solution by reducing temperature in the reboiler. This will cause the rate of feed to have a smaller effect on the process compared to what could be expected. Secondly, the decrease of CO_2 loading in solution is not so significant before and after treatment during the measuring time. Normally, the CO_2 loading can decrease 0.01 – 0.1 mol/mol after treatment with ultrasound, from originally 0.2 – 0.4 mol/mol. The CO_2 stripping depends very much on the amount of free CO_2 in the solution, the fresh rich solution that comes into the reboiler may not be taking much free CO_2 into the reboiler solution.

Therefore, the significance of variables as obtained via statistical analysis, can be summarized as

1) CO_2 loading: positive response, strong effect
2) Interaction of ultrasound intensity and CO_2 loading: positive response "middle" size effect
3) Intensity of ultrasound: positive response, "middle" size effect
4) Frequency of ultrasound: positive response, "middle" size effect
5) Temperature (and hence pressure): negative response, "middle" size effect
6) On-stream time of ultrasound and CO_2 loading: positive response, "middle" size effect
7) On-stream time of ultrasound: positive response, "middle" size effect
8) The rest variables are "small" size effects

5.5. Specific energy consumption as the dependent variable

The relative effects of variables on the specific energy consumption (E_s) for CO_2 stripping enhanced by ultrasound were obtained, and the significant variables were identified. E_s includes both steam heat and ultrasound energy input. The results are shown in Figure 13. Note that experiments 2 and 8 had, as previously, to be excluded from the analysis to be able to correlate the E_s to the independent variables. In the figure, higher absolute value of weighted regression coefficient indicates higher impact on the energy consumption, and a negative value of the weighted regression coefficient means that the variable results in a low the energy consumption, has a positive effect on energy saving.

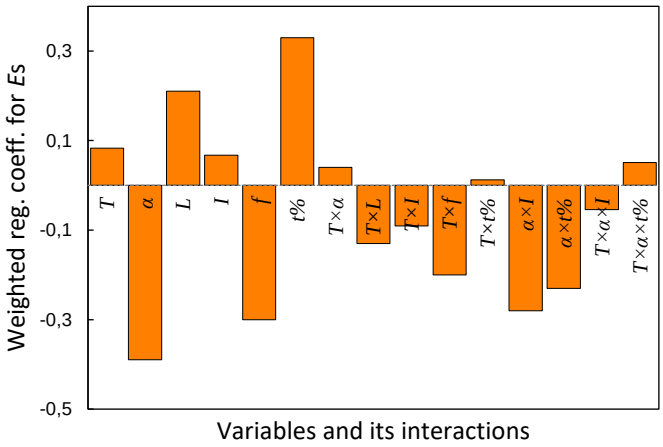

Figure 13. Effects of the variables and its interactions on the specific energy consumption, E_s.

As was found for the case of A_{CO2} as the dependent variable, the CO_2 loading is also here the most important parameter. For specific energy consumption, however, this is a negative (although positive for reducing energy) parameter, that is, a higher CO_2 loading in the rich solution results in lower energy consumption when the solution was treated by ultrasound.

The weighted regression coefficient value of temperature (pressure) is positive, which means it has a negative effect on saving energy. This result is opposite to our previous experiments at ambient pressure.[11] Because the higher pressure will depress the formation and growth of bubbles, even

though a higher temperature leads to higher chemical reaction rate for producing CO_2 from carbamates. Therefore, the combined effect of temperature and pressure is negative on E_s. More studies of the effects of pressure on the CO_2 stripping can be found in our previous work.[12]

Comparing the effects of variables in Figure 12 and Figure 13, it can be found that most variables and the interactions have the same effect trends on A_{CO2} and E_s, because in general the higher CO_2 stripping rate in the process will achieve lower energy consumption. However, there are some parameters such as L, I and t%, where higher the values of them lead to higher CO_2 stripping rates, but also result in higher energy consumption. This means that it is more important to find the optimized values of these variables in order to achieve a low energy consumption for CO_2 stripping.

5.6. Relationship of dependent variables

Figure 14 shows the established correlation between the specific energy consumption and the CO_2 stripping rate. There is (as expected) a negative correlation between the two responses A_{CO2} and E_s, implying that when the operational condition is optimum, high CO_2 stripping rate with low energy input can be obtained.

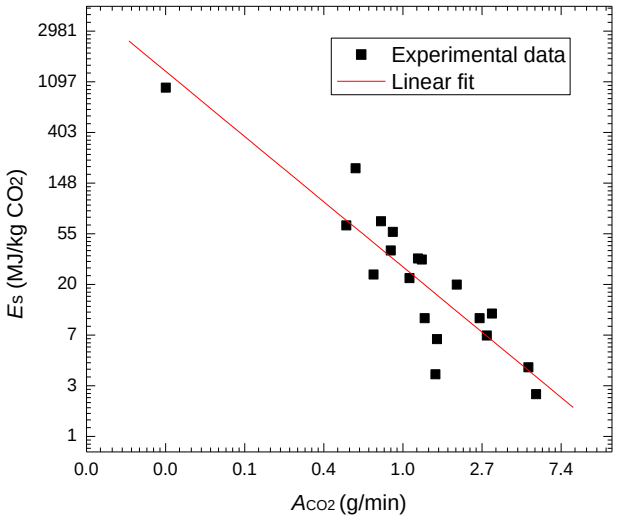

Figure 14. Established correlation between specific stripping energy and the CO_2 stripping rate.

6. Conclusions

The use of ultrasound to intensify the desorption of CO_2 from loaded solutions was investigated covering a typical industrial case of a pressure range from 0 to 1.5 barg. The effects of six variables i.e., temperature (T), intensity of ultrasound (I), frequency of ultrasound (f), percentage on-stream time of ultrasound (t%), liquid flow rate (L) and CO_2 loading (α), and their interactions were studied. Based on the design test matrix and experimental results, a PLS method was employed to analyze the

effects of the variables on two dependents the CO_2 stripping rate (A_{CO2}) and specific energy consumption (E_s).

The results show that the enhancement of the CO_2 stripping rate by ultrasound is significant and an improvement of magnitudes 400% can be achieved, indicating that the mass transfer can be intensified significantly by ultrasound. Compared to the treatment by heat only, the best energy saving achieved was 36% by using ultrasound + heat treatment when the CO_2 loading is high, and the specific energy consumption found was 2.3 MJ/kg CO_2.

Modelling and correlations based on the test matrix results were done with PLS method to find the effects of various variables. A model explaining 87.5 % of the variation in the rate of CO_2 stripping (A_{CO2}) is obtained by a PLS method, and the model explains 87.6 % of the specific energy consumption (E_s). Analysis of variables shows that the variables such as CO_2 loading, temperature / pressure and ultrasound parameters are important to energy consumption. The CO_2 loading is the significant positive effect variable, temperature / pressure is negative on energy saving and CO_2 stripping rate and ultrasound parameters have varied effects on the dependents. The analysis shows that there is scope for optimizing ultrasound energy input.

■ ASSOCIATED CONTENT

Supporting Information

Uncertainty analysis, photo of the typical sonotrodes for the experiments and variable analysis

■ AUTHOR INFORMATION

Corresponding Author

*E-mail: jiru.ying@sintef.no

■ ACKNOWLEDGMENTS

Funding: This work was supported by Shell Technology Norway AS (No. SC14001) and Norwegian Research Council (No.235055).

■NOMENCLATURE

Abbreviations

RNH_2 = monoethanolamine (MEA) in this work

Parameters and Variables

a, is constant item in the equation (13)

A_{CO2}, is the CO_2 stripping rate in the reboiler, g/min

b_i, represents the parameter of ith variable in the equation (13)

H, is the total energy consumption in the process, MJ/min

H_{cw}, is the energy requirement for vapor condensed, which calculated by cooling water, MJ/min

H_{st}, is the energy input by steam heat, MJ/min

H_{US}, is the ultrasound energy input, MJ/min

E_s, is the specific energy consumption, MJ/kg CO_2

$E_{s,H}$, is the specific energy consumption when CO_2 stripping only by heat in the experiment, MJ/kg CO_2

$E_{s,US}$, is the specific total potential ultrasound energy consumption, MJ/kg CO_2

f, is the frequency of ultrasound, kHz

I, is the intensity of ultrasound (full intensity is 500 W), %

L, is the liquid flow rate input in the reboiler, m^3/s

P, is the pressure in the reboiler, bar(g)

P_{liq}, is the liquid pressure at the site in a solution, Pa

P_s, is the pressure caused by surface tension outside of the bubble in a liquid, Pa

P_{CO2}, is the partial pressure of CO_2 in the bubble, Pa

P_{vap}, is the solvent vapor pressure in the bubble, Pa

R, is the diameter of a bubble in equation (2), m

R, is gas constant, J/K mol

t_{on}, on-stream time of ultrasound in a period, s

t_{off}, off-stream time of ultrasound in a period, s

t%, percentage of on-stream time of ultrasound in a period, %, $t\% = t_{on} /(t_{on} + t_{off}) \times 100\%$

T, is the temperature in the reboiler, ^oC

x_i, represents the ith variable in the equation (13)

Greek Symbols

α, is the CO_2 loading in the aq. MEA solution, mol CO_2/mol MEA

σ, is the surface tension produced by the liquid around a bubble, N/m

η, is the energy saving due to using ultrasound in the reboiler process, %

References

1. Mason, T. J., *Advances in Sonochemistry*. JAI Press: 1999; Vol. 5.

2. Brennen, C. E., *Cavitation and bubble dynamics*. Cambridge University Press: 2013.

3. Pilli, S.; Bhunia, P.; Yan, S.; LeBlanc, R.; Tyagi, R.; Surampalli, R., Ultrasonic pretreatment of sludge: a review. *Ultrasonics sonochemistry* **2011,** *18* (1), 1-18.

4. Lepoint, T.; Mullie, F., What exactly is cavitation chemistry? *Ultrasonics Sonochemistry* **1994,** *1* (1), S13-S22.

5. Stephanis, C.; Hatiris, J.; Mourmouras, D., The process (mechanism) of erosion of soluble brittle materials caused by cavitation. *Ultrasonics sonochemistry* **1997,** *4* (3), 269-271.

6. Eskin, D.; Al-Helal, K.; Tzanakis, I., Application of a plate sonotrode to ultrasonic degassing of aluminum melt: acoustic measurements and feasibility study. *Journal of Materials Processing Technology* **2015,** *222*, 148-154.

7. Gantert, S.; Möller, D., Ultrasonic desorption of CO2–a new technology to save energy and prevent solvent degradation. *Chemical Engineering & Technology* **2012,** *35* (3), 576-578.

8. Xue, J.; Shen, B.; Du, S.; Lan, X., Study on desorbing sulfur dioxide from citrate solution by ultrasonification. *Chinese Journal of Chemical Engineering* **2007,** *15* (4), 486-491.

9. Zhang, J.; Qiao, Y.; Agar, D. W., Intensification of low temperature thermomorphic biphasic amine solvent regeneration for CO 2 capture. *Chemical Engineering Research and Design* **2012,** *90* (6), 743-749.

10. Tanaka, K.; Fujiwara, T.; Okawa, H.; Kato, T.; Sugawara, K., Ultrasound irradiation for desorption of carbon dioxide gas from aqueous solutions of monoethanolamine. *Japanese Journal of Applied Physics* **2014,** *53* (7S), 07KE14.

11. Ying, J.; Eimer, D. A.; Haugen, H. A., Ultrasound to assist desorption of CO2 from loaded monoethanolamine solutions. In *14th Meeting of the European Society of Sonochemistry*, Avignon, France, 2014; pp 235-236.

12. Ying, J.; Haverkort, J.; Eimer, D. A.; Haugen, H. A., Ultrasound enhanced CO2 Stripping from Lean MEA Solution at Pressures from 1 to 2.5 bar (a). *Energy Procedia* **2017,** *114*, 139-148.

13. Kraus, E. B.; Businger, J. A., *Atmosphere-ocean interaction*. Oxford University Press New York: 1994; Vol. 2.

14. Schueller, B. S.; Yang, R. T., Ultrasound enhanced adsorption and desorption of phenol on activated carbon and polymeric resin. *Industrial & engineering chemistry research* **2001,** *40* (22), 4912-4918.

15. Caplow, M., Kinetics of carbamate formation and breakdown. *Journal of the American Chemical Society* **1968,** *90* (24), 6795-6803.

16. Ying, J.; Eimer, D. A., Determination and measurements of mass transfer kinetics of CO2 in concentrated aqueous monoethanolamine solutions by a stirred cell. *Industrial & Engineering Chemistry Research* **2013,** *52* (7), 2548-2559.

17. Peregrine, D., The Acoustic Bubble. By TG LEIGHTON. Academic Press, 1994. 613 pp.£ 95. ISBN 0-12-441920-8. *Journal of Fluid Mechanics* **1994,** *272*, 407-408.

18. Doinikov, A. A., Bjerknes forces and translational bubble dynamics. *Bubble and particle dynamics in acoustic fields: modern trends and applications* **2005,** *661*, 95-143.

19. Coulson, J.; Richardson, J.; Backhurst, J.; Harker, J., *Chemical engineering*. 6 ed.; Elsevier: 1999; Vol. 1.

20. Box, G. E.; Hunter, J. S.; Hunter, W. G., *Statistics for experimenters: design, innovation, and discovery*. Wiley-Interscience New York: 2005; Vol. 2.

21. Rochelle, G.; Chen, E.; Freeman, S.; Van Wagener, D.; Xu, Q.; Voice, A., Aqueous piperazine as the new standard for CO2 capture technology. *Chemical engineering journal* **2011,** *171* (3), 725-733.

22. Geladi, P.; Kowalski, B. R., Partial least-squares regression: a tutorial. *Analytica chimica acta* **1986,** *185*, 1-17.